AD/A-004 954

FIBERGLASS-REINFORCED-POLYESTER LAMINATE FOR USE IN PROTECTIVE STRUCTURES

G. Warren

Civil Engineering Laboratory (Navy)
Port Hueneme, California

January 1975

UNCLASSIFIED

SECURITY CLASSIFICATION OF THIS PAGE (When Data Entered)

REPORT DOCUMENTATION PAGE	READ INSTRUCTIONS BEFORE COMPLETING FORM
1 REPORT NUMBER: TR-318	2 GOVT ACCESSION NO. / 3 RECIPIENT'S CATALOG NUMBER: AD/A-002954
4 TITLE (and Subtitle): FIBERGLASS-REINFORCED-POLYESTER LAMINATE FOR USE IN PROTECTIVE STRUCTURES	5 TYPE OF REPORT & PERIOD COVERED: Not final; 51-037
	6 PERFORMING ORG. REPORT NUMBER
7 AUTHOR(s): G. Warren	8 CONTRACT OR GRANT NUMBER(s)
9 PERFORMING ORGANIZATION NAME AND ADDRESS: Civil Engineering Laboratory, Naval Construction Battalion Center, Port Hueneme, CA 93043	10 PROGRAM ELEMENT, PROJECT, TASK AREA & WORK UNIT NUMBERS: 63765M; USMC PO-3-0022; 51-037
11 CONTROLLING OFFICE NAME AND ADDRESS: Marine Corps Education and Development Command, Quantico, VA 22134	12 REPORT DATE: January 1975
	13 NUMBER OF PAGES: 31
14 MONITORING AGENCY NAME & ADDRESS (if different from Controlling Office)	15 SECURITY CLASS (of this report): Unclassified
	15a DECLASSIFICATION/DOWNGRADING SCHEDULE

16 DISTRIBUTION STATEMENT (of this Report)

Approved for public release; distribution unlimited.

17 DISTRIBUTION STATEMENT (of the abstract entered in Block 20, if different from Report)

18 SUPPLEMENTARY NOTES

PRICES SUBJECT TO CHANGE

19 KEY WORDS (Continue on reverse side if necessary and identify by block number)

modular protective structures, fiberglass-reinforced-polyester laminates, military ground targets, ammunition GRP modules, fortifications, military personnel

20 ABSTRACT (Continue on reverse side if necessary and identify by block number)

This report presents the testing and behavioral study program leading to the development of structural design criteria for a fiberglass-reinforced-polyester (GRP) laminate. This study is a part of the Civil Engineering Laboratory's effort to develop, test, and evaluate a modular protective construction system for the Marine Corps. The Marine Corps system is to employ GRP modules as reusable elements for rapid construction of temporary protection for military ground targets against conventional weapon threats.

continued

DD FORM 1 JAN 73 1473 EDITION OF 1 NOV 65 IS OBSOLETE

UNCLASSIFIED

SECURITY CLASSIFICATION OF THIS PAGE (When Data Entered)

Block 20. Continued

The GRP laminate consists of a polyester resin (22% by weight) reinforced with plies of fiberglass woven fabric.

The objective of the test program was to determine and evaluate the mechanical characteristics of the GRP through a series of flexural, tensile, compressive, and shear tests. In addition, more efficient uses of the structural strength of the GRP were investigated whereby the GRP laminate sheets were employed as facings of sandwich plates. Employing the GRP in sandwich configurations increased the structural resistance while increasing fabrication costs and shipping cube (volume).

Because of its superior ballistic resistance, the GRP was selected for the Marine Corps protective construction program; however, the laminate is inherently weak in compression and is highly susceptible to creep, localized buckling, and moisture. The established criteria will provide design guidance for GRP structural components of protective structures. The criteria will be used to predict structural behavior, load limits, failure modes, and usable life of GRP structures. In addition, the efficient use of the mechanical properties of the GRP can be used as one criteria for evaluating future candidate modular systems.

Library Card

Civil Engineering Laboratory
FIBERGLASS-REINFORCED-POLYESTER LAMINATE FOR USE IN PROTECTIVE STRUCTURES (Not final), by G. Warren
TR-818 28 p. illus January 1975 Unclassified

1. Modular protective structures 2. Military ground targets I. 51-037

This report presents the testing and behavioral study program leading to the development of structural design criteria for a fiberglass-reinforced-polyester (GRP) laminate. This study is a part of the Civil Engineering Laboratory's effort to develop, test, and evaluate a modular protective construction system for the Marine Corps. The Marine Corps system is to employ GRP modules as reusable elements for rapid construction of temporary protection for military ground targets against conventional weapon threats. The GRP laminate consists of a polyester resin (22% by weight) reinforced with plies of fiberglass woven fabric.

Because of its superior ballistic resistance, the GRP was selected for the Marine Corps protective construction program; however, the laminate is inherently weak in compression and is highly susceptible to creep, localized buckling, and moisture. The established criteria will provide design guidance for GRP structural components of protective structures. The criteria will be used to predict structural behavior, load limits, failure modes, and usable life of GRP structures. In addition, the efficient use of the mechanical properties of the GRP can be used as one criteria for evaluating future candidate modular systems.

CONTENTS

INTRODUCTION AND OBJECTIVE

The Civil Engineering Laboratory (CEL) has been evaluating a highly fragment-resistant armor material for the Marine Corps. If used in a reuseable modular component design this material, GRP,* could be used in forward areas to assemble a family of shelters easily and quickly for protecting ground targets against effects from conventional weapons. Present systems use sandbags, metal components, concrete elements, or timber construction requiring long erection time. Although such systems provide adequate protection after erection, little protection is afforded the erectors during the long periods of construction.

With a reuseable module and reduced erection time, combat troops can be redirected from protective construction to their primary mission; the final goal is to provide an alternative to sandbag, concrete, or timber construction.

Personnel, aircraft, fuel, and ammunition are typical targets to be protected by the modular fortification system from conventional weapons, such as mortars, artillery, rockets, and general purpose bombs. Effects from the weapons include fragmentation and impulse blast loading. Previous investigations have demonstrated that the GRP is an effective deterrent to fragments [1,2].

Since the modular components must resist blast effects in addition to fragmentation, the GRP components must be structurally reliable, thus requiring an evaluation of the mechanical properties of the GRP laminate. The GRP structures must also be capable of sustaining other loading:

1. Dead weight

2. Soil loading (the structures are to be ballistically upgraded by adding soil in wall cavities between panels)

3. Wind loading (the structures must be able to resist wind loading from a hovering helicopter)

4. Live loading (the roofs and walls must support personnel and equipment during and after erection)

A test program was undertaken to establish the structural properties of the GRP laminate, evaluate failure mechanisms, and recommend efficient GRP structural configurations.

GRP Laminate Description

The GRP laminate was prepared from layers of fiberglass woven cloth surrounded by a matrix of polyester resin. The resin, which conformed to MIL-R-21067, contained 70% by weight of thermosetting polyester with the remainder of the formula being monomeric styrene.

The glass woven fabric conformed to Style 1157 (manufacturer's specifications, see Figure 1). This particular fabric weighed 24 ounces per square yard and consisted of electrical glass composition (E-glass) with a continuous filament of 0.00037-inch nominal diameter in both the warp and fill rovings. Each filament of the rovings (groups of filaments) is nominally 13,500 yards per pound. Each roving was composed of 60 filaments. There were 5 rovings (ends) per inch in the warp direction of the cloth and 4 rovings (picks) per inch in the fill direction. The finish on the cloth was a starch binder.

The laminate was prepared by using 48 plies of the above cloth in the resin matrix per inch thickness of laminate. The GRP was cured by the manufacturer for 2 hours at 200°F and 100 psi pressure. A cross section of the GRP is shown in Figure 2. The laminate's density was 0.071 pound per cubic inch (1.97 specific gravity). Samples of the laminate were tested in accordance with Method 7061 of Federal Test Method Standard No. 406 and found to consist of 21.76% resin by weight. This is a very low resin content for a laminate used in structural applications; however, tests have indicated that 20% resin content is optimum for best fragmentation resistance.

* Fiberglass-reinforced polyester, the fiberglass is woven roving design.

Table 1. GRP Coupon Tests for Material Properties

Stress Mode	Test	Laminate Thickness (in.)	Anistropic Direction
Room-Conditioned Specimen			
Tension	ASTM D638	1/4, 1/8	fill, warp
Compression	CEL[a]	1/4	fill
Flexure	ASTM D790	1/4	fill, warp
Laminating Shear	CEL[a]	1/4	fill
Punching Shear	ASTM D732	1/4	perpendicular to laminate sheet
Water-Soaked[b] Specimen Tested at Room Temperature			
Tension	ASTM D638	1/4, 1/8	fill, warp
Compression	CEL[a]	1/4	fill
Flexure	ASTM D790	1/4	fill, warp

[a] CEL-designed specimen tested at strain rates recommended by ASTM.

[b] Water-soaked 24 hours as specified by ASTM.

Test Program

A series of coupon tests was conducted to evaluate strength and behavior characteristics and to establish design criteria for the laminate. The information was required to design the components of the protection system to utilize fully both the structural and ballistic properties of the laminate. The coupon test program is given in Table 1. It included tensile, compressive, flexural, laminate shear, and punching shear tests. From the coupon tests the following properties were determined: elastic modulus, yield strength, maximum strength, stress-strain behavior, and energy absorption properties. In addition to the above tests, two tensile and two compression test specimens were strain-gaged in order to obtain Poisson's ratio.

After completion of the coupon tests and evaluation of the behavioral characteristics, a series of single- and four-point loaded flexural tests were conducted on six sandwich configurations employing GRP sandwiched with aluminum honeycomb core.

COUPON TESTS OF GRP LAMINATE

Summaries of the results from the room-conditioned tests are tabulated in Table 2. Typical resistance-deformation curves for the various types of tests are presented in Figures 3 through 7.

During initial stages of loading in all stress modes, the behavior of the laminate was governed by the properties of the polyester resin. After the resin strength was exceeded, the fiberglass characteristics controlled the laminate behavior.

The GRP exhibited a considerable amount of ductility after yield or maximum stress was attained in all stress modes except, notably, the tensile mode where failure of the fiberglass tended to be sudden and complete. Specimens subjected to stress modes wherein large ductility occurred were not loaded to complete collapse; instead, they were deformed to a particular strain level to which the material would be subjected during "field" use. Load-deformation curves in Figures 5 and 6 give a good indication of the GRP ductility.

There were different load-carrying characteristics associated with the warp and fill directions of the laminate since there was 20% more fiberglass in the warp direction than in the fill direction. As might be anticipated, on the basis of tensile and flexural tests, the warp direction had greater ultimate (maximum) strength (10% tensile and 4% flexural). All of the values given in the following paragraphs are for the fill direction and 1/4-inch thickness (room-conditioned tests) unless otherwise noted. It is recommended that the structural design properties be based on those associated with the fill direction of the laminate (Table 2).

From the strain-gaged coupon specimens, Poisson's ratio was determined to be approximately 0.1.

Test Results for Specific Stress Modes

Tension. Example curves of coupon tensile load deformation are given in Figures 3 and 4. A tested tensile coupon specimen is shown in Figure 8 where the deteriorated resin delaminated from the fiberglass, characteristic of the tensile failure mode.

Although the GRP did not exhibit ductility in tension, it did provide a higher level of strain energy absorption than was characteristic of the compression

Table 2. Properties of GRP Laminate[a]

(Poisson's Ratio = 0.1.)

Property	Stress Mode				
	Tension	Compression	Flexure	Laminating Shear	Punching Shear
Initial Stress Modulus (psi)	2.55×10^6	1.72×10^6	1.55×10^6	0.38×10^6	0.15×10^6
Secondary Stress Modulus (psi)	1.78×10^6	–	–	–	–
Stress at Resin Failure (psi)	8,800	6,000	6,500	820	19,300
Maximum Stress (psi)	40,000	6,000	6,500	–	19,300
Yield Strain (in./in.)	0.0035	0.007	0.004	0.0022	0.130
Rupture Stress (psi)	40,000	2,400	3,200	–	7,600
Rupture Strain (in./in.)	0.025	0.10	0.026	–	–
Elastic Strain Energy (psi-in./in.)	15	22	13	1	1,250
Total Strain Energy (psi-in./in.)	520	240	80	–	–

[a] 1/4-inch, room-conditioned, fill direction.

or flexural stress modes (Table 2). The tests indicated an initial tensile modulus of 2.55×10^6 psi to a stress level of 8.8 ksi, at which point the resin apparently began to break down; there was also a load-resistance transition to the fiberglass. The transition modulus was 1.38×10^6 psi to a stress level of 17.9 ksi. Then the modulus was 1.78×10^6 ksi until an ultimate strength of 40.0 ksi was reached. Failure occurred in a stepwise fashion as groups of fiberglass strands were broken, and the load-carrying capacity dropped eventually to zero with increased strain. Strain at maximum resistance was 0.025 and was 2 to 4 times this amount at complete collapse.

Compression. Due to the instability of the GRP, the compression coupon specimen (see Figure 9) was cut from a sandwich prepared from 1/4-inch-thick laminate facings cemented to 3/4-inch-thick aluminum honeycomb core. The compressive strength of the core was negligible. The specimen width was 1 inch and length was 1-1/2 inches. Before testing, specimens were capped with a polyester resin in order to insure uniform compressive loading.

Example load-deformation curves for compression are shown in Figure 5. A typical failure mechanism is shown in the photograph in Figure 10. The elastic compression modulus was 1.72×10^6 psi to a maximum loading of 6.0 ksi where the laminate resin broke down. The load-carrying capacity gradually dropped off to 40% of the maximum and held at this level until a strain of 0.10 was reached when the tests were terminated.

Breakdown of the resin resulted in a diagonal crack (Figure 10). As the resistance dropped off and further strain was experienced, slippage occurred along the crack, and the glass fibers across the crack were subjected to tensile stresses. Thus, the woven cloth plies in the vicinity of the crack delaminated and buckled with continued specimen deformation (Figure 10). The compressive failure was a localized shearing type, resulting in considerable strength reduction. The relatively low compression strength was due to the low resin content in the laminate. Further deformation of the compression specimen resulted in localized strain near the crack accompanied by relaxation of strain elsewhere as the load resistance dropped.

Flexure. The flexural properties of the laminate were governed by its compressive capacity. Another factor was the support conditions of the specimen. Photographs of GRP coupon flexural failures are presented in Figure 11. Sample test curves of flexural resistance to deformation are given in Figure 6. From the coupon tests, the laminate showed a flexural elastic modulus of 1.55×10^6 psi to a maximum stress of 6.5 ksi (strain at maximum loading was approximately 0.004).

After attaining the maximum resistance, the laminate resin began to break down and a diagonal crack was formed in the compression zone of the specimen cross section (Figure 11). The load resistance dropped to 40 to 60% of maximum as the fiberglass strands were subjected to tensile action as slippage occurred along the crack. Just as in the compression mode, localized buckling and delamination occurred in the vicinity of the crack as deformation was continued.

The behavior of the specimen after breakdown of the resin and the subsequent drop in load-carrying capacity depended on the end supports. For the case of roller supports, the specimen continued to deflect while carrying approximately the same loading (40 to 50% maximum). However, for the case of pinned supports at both ends, the load resistance increased up to near maximum resistance with continued deformation. This was attributed to the tensile membrane resistance of the laminate. In any case, the laminate is capable of deformation (hinge rotation) in excess of 12^0 about the support without collapse and maintaining at least 40% of the maximum loading. The test results shown in Figure 6 are from specimens on roller-type end supports.

Shear. Both punching and lamination shear tests were performed. Lamination shear tests were performed using the notched type of tension-loaded specimen shown in Figure 12 (using 1/4-inch-thick laminate). This specimen was considered to provide a lower bound to the lamination shear strength since it was virtually impossible to eliminate all the eccentricity in loading. Results indicated a linear stress-strain response until resin breakdown which produced a crack between woven roving plies extending between the two sawed notches on the specimen (Figure 12). Tests were terminated at this point. The elastic modulus of lamination shear was 0.38×10^6 psi and the maximum lamination shear strength was 820 psi.

Punching shear tests produced linear resistance-deformation response up to resin breakdown after which there was a gradual decrease in the load-carrying capacity (Figure 7). The elastic modulus for punching shear was 0.15×10^6 psi and the maximum shear strength was 19.3 ksi. This mode of stress exhibited the highest level of elastic strain energy. Just as in the compression and flexural modes, after resin deterioration, the fiberglass could not sustain the maximum shear resistance level; and delamination resulted after the glass was subjected to tension across the failure crack.

Parameter Effect on Structural Properties

Water Adsorption. Specimens of each stress mode except lamination shear were also tested after being immersed 24 hours in water. Typical resistance-deformation curves are plotted in Figures 3 through 6 along with the room-conditioned test results.

After being immersed in water for 24 hours, the GRP laminate specimens were observed to absorb water at 1.5 to 2.0% by weight (uncoated specimens). Because of the low resin content and the starch binder, the laminate was more susceptible to strength deterioration due to water absorption. Load resistance decreased from 30 to 60%. The effect is illustrated in Figures 3 through 6. The water absorption tends to break down the bond between the polyester resin and the fiberglass strands. It was noted, however, that the tests indicated little decrease in the GRP's ductility due to water absorption.

Due to the detrimental effect of moisture, a coating will be required if the GRP is to retain its structural and ballistic integrity in a humid environment.

Thickness of GRP. On the basis of coupon tensile tests, both dry and water-immersed, the thinner laminates exhibited slightly less strength and were more deteriorated by water absorption. The 1/8-inch laminate decreased more in strength from the 24-hour water immersion than did the 1/4-inch laminate.

Capacity for Reloading and Reverse Loading. Flexural coupons (and later sandwich flexural specimens) were subjected to reloading after inducing permanent deformation and exceeding maximum stress level. The reload-deformation relationship was linear (much less stiff, however, than the original stiffness) and returned to the level of resistance at which the load-carrying capacity was originally dropped. These specimens continued to deform as if the load had never been removed.

Reverse flexural loading was applied by, first, deforming the specimen beyond the maximum load-carrying capacity in one direction, and then turning the beam specimen over and applying load in the opposite direction. The behavior of the specimen was similar to that of the reloaded specimens. The load deformation was linear to a maximum resistance and then leveled. If 12 degrees of rotation has not been exceeded in the original loading direction, it could be deformed this amount in the opposite direction. However, if 12 degrees of rotation was exceeded in the initial loading, the specimen could carry little loading in the opposite direction. The fibers in the laminate originally loaded in compression were generally broken after 12 degrees of hinge rotation.

SANDWICH TESTING

Sandwich construction is the most efficient method of utilizing the structural capability of the GRP. Facings are spaced some distance apart where they will be subjected to in-plane loading for resisting bending and membrane forces. Separating the facings with lightweight core material (aluminum honeycomb) achieves a high ratio of stiffness to weight. The core is designed to resist shear and to stabilize the facings through a bonding adhesive medium. Sandwich construction is inherently more costly in fabrication and will increase the shipping cube (volume).

Six GRP sandwich construction configurations (Figure 13) were considered and tested. Configuration 1 uses the GRP as a core material and is considered to have the poorest ratio of structural strength to weight. The other five utilize a lightweight honeycomb core and GRP laminate facings. The sandwich configurations that utilized aluminum or reinforced epoxy possessed the greatest ratio of ultimate strength to weight.

Sandwich Tests and Results

Sandwich plates were fabricated in the configurations shown in Figure 13. The plates measured 12 x 12 inches, 18 x 18 inches, and 18 x 48 inches and were fabricated by CEL technicians (Figure 14). After curing, the plates were cut into flexural specimens in widths approximately equal to thicknesses. Sandwich specimens were tested either to failure or to a stable resistance level, using single- and four-point loading configurations (Figure 15).

A summary of the results of the sandwich flexural tests are presented in Table 3. Example resistance-deformation curves are presented in Figures 16 through 24. Photographs of example failure mechanisms are shown in Figures 25 through 33.

Evaluation of Sandwich Behavior

The GRP in sandwich construction exhibited properties similar to those exhibited during the coupon testing. The amount of deterioration from moisture absorption is shown in the resistance-deflection curve in Figure 19, as compared to Figure 18. The tensile membrane contribution to the resistance beyond elastic limits is shown in the resistance curve shown in Figure 20, as compared to Figure 17. The compression failure mechanism of a GRP sandwich facing is shown in Figure 32 and is similar to the coupon compression failure shown in Figure 10.

All sandwich configurations exhibited an elastic range, with the greater stiffnesses associated with the more complex sandwich configurations. With the exception of Configuration 3, the behavior of the sandwiches in the linear elastic range presented few material problems from buckling or delamination of facings. Fabrication difficulty (low bonding pressure and temperature) of specimens of Configuration 3 resulted in delamination of the components at load resistances below those expected (Figure 25). A premature facing delamination of a Configuration 5 specimen is shown in Figure 26. Failure of the adhesive in the elastic range was particularly sudden and was accompanied by a large loss in load-carrying capacity (Figure 21).

The strength of the adhesive and its flexibility is dependent upon the sandwiching procedure; that is, mixture of adhesive components, thickness and

Table 3. Summary of Sandwich Tests

Configuration	Experimental Values						Predicted Values	
	Compression Face Thickness (in.)	Tension Face Thickness (in.)	Core Thickness (in.)	Yield Moment (in.-lb)	EI (lb-in.^{2} x 10^6)	Maximum Moment (in.-lb)	Yield Moment (in.-lb)	$(EI)_p$ (lb-in.^{2} x 10^6)
1	1/16	7/16	1/16	1,224	0.097	1,694	1,310	0.078
2	1/4	3/4	1/4	2,875	0.362	2,850	1,500	0.260
3	5/16	2	5/16	10,707[a]	2.829	10,707	8,670	2.836
4	1/16	3/4	1/4	2,080	0.270	2,920	1,990	0.260
5	1/8	3/4	1/4	3,400	0.263	3,420	6,940	0.199
6	1/4	3/4	1/16	2,040	0.287	2,880	1,990	0.260

[a] Maximum attained value before premature adhesive failure.

evenness of the adhesive layer, and the amount of residual stresses produced by the curing temperature and pressure. The results of the tests involving Configuration 3 indicate adhesive joints should be kept to a minimum and the choice of adhesive carefully considered in order to sustain the desired load capacity and be capable of attaining large ductile strains.

Several premature shear and buckling failures in the core material were encountered; however, they were not as sudden and complete as the adhesive failures. The core-buckling failure of Configuration 4 is shown in Figure 27.

Beyond the elastic range, buckling and delamination of the compression facings were the usual failure modes of the sandwiches. However, except for premature adhesive breakdown, the failure of Configuration 3, and the behavior of Configuration 5, the sandwiches generally exhibited a very ductile flexural mode. A failure of Configuration 5 is shown in Figure 31. Due to the brittleness of the reinforced epoxy used in the compression face, the failure of the sandwich was quite sudden and complete as shown in the resistance-deflection curve in Figure 23.

With the nonsymmetrical sandwich Configurations 4, 5, and 6, the behavior beyond the elastic range was governed by the sandwich facings that initially yielded. This was particularly true for Configuration 6 in which the GRP facing was in compression. As deomnstrated in Figure 24, when the GRP yielded first (Figure 32), the load-resistance reduced to approximately half of the maximum loading, after which the load-resistance leveled off. When the aluminum facing initially yielded, as in Configuration 6, the resistance leveled off and maintained the maximum load (Figure 24) until the aluminum failed (Figure 33). The latter type of failure resulted in a sudden and complete resistance loss similar to that with Configuration 5.

If the adhesive which bonded sandwich components was correctly applied and was capable of sustaining the necessary strain energy absorption of the facings, sandwich Configurations 2, 3, and 4 presented the most desirable structural characteristics. Configuration 1 lacked the high level of strength-to-weight, and the brittleness of the reinforced epoxy limited the ductility of Configuration 5.

Comparison of Predicted and Experimental Properties

Tabulated in Table 3 are the predicted and experimentally calculated stiffnesses, $(EI)_p$ and $(EI)_e$, respectively for the tested sandwich configurations. The predicted stiffnesses were obtained by

1. Using the GRP material properties tabulated in Table 2.

2. Using the manufacturer's recommended mechanical properties for aluminum and the fiberglass-reinforced epoxy.

3. Assuming that the flexural loading was resisted by the sandwich facings only.

4. Assuming uniform tensile and compressive stress across the facings' sections.

5. Assuming flexural yielding in one of the sandwich facings prior to any localized buckling or shear failure in the core or adhesive joint.

The predicted stiffness of the sandwiches, $(EI)_p$, was obtained from the experimentally obtained strain characteristics of the GRP laminate and other facing materials and the expression

$$\rho = \frac{M}{(EI)_p} = \frac{\epsilon_t + \epsilon_c}{h}$$

where ϵ_t and ϵ_c are the predicted strains at the centroid of the tensile and compressive facings, respectively, while the sandwich beam is subjected to the moment M. The moment arm length between the centroids of the tensile and compressive forces is designated as h.

The predicted yield moment, M_y, was calculated from

$$M_y = f_y t h$$

where t is the thickness of the facing that yielded first (or the thickness of the GRP if it attained maximum stress in compression), and f_y is the yield stress of the material used in the facing (or the maximum GRP compressive stress). The value for $f_y t$ was determined for each facing, and the lesser of the two was used to determine M_y.

The experimental values of the elastic stiffness, $(EI)_e$, were calculated from the linear portions of the load-deformation curves and the expressions:

$$(EI)_e = \frac{P}{\Delta}\left(\frac{L^3}{48}\right) \quad \text{for single-point loading}$$

$$(EI)_e = \frac{P}{\Delta}\left(\frac{63\,L^3}{4,000}\right) \quad \text{for four-point loading}$$

where Δ is the deflection measured at the beam specimen midpoint and P is the force applied by the machine head.

Linear behavior of the various sandwich configurations compare reasonably well with the predicted behavior (Table 3). The behavior beyond the elastic range was dependent in several cases on the buckling and shear strength of the core and laminating strength of the adhesive. The strength of the adhesive joint adjacent to an aluminum sheet facing surface was particularly susceptible to premature failure (both before yield and after large strain) and was unpredictable. Thus, no attempt was made to extend predicted calculation beyond the elastic range.

Creep Tests

The GRP laminate has been shown to be susceptible to continuous creep [3]. Two flexural specimens of Configurations 2 and 4 were exposed to long-term loading at room conditions with a point load of 264 pounds (0.5 P_y for Configuration 2 and 0.6 P_y for Configuration 4). The loading arrangement is shown and results are plotted in Figure 34.

Within the first 125 hours the specimens had deflected in creep 20% of the initial deflection. Beyond 125 hours the rate of creep was constant. Although not tested, it was believed that much of the GRP creep would be eliminated by the employment of aluminum sheets in both facings of the sandwich (Configuration 3).

CANDIDATE SANDWICH PANEL MODULES

A good comparison between predicted and experimentally obtained properties justified the use of the same predicting procedure to obtain load-

deformation curves for possible sandwich candidates for the modules of the protective construction program. In order to structurally compare the six sandwich configurations, the following materials and quantities were considered in the candidate sandwich modules:

1. 1/2-inch (or two 1/4-inch sheets) of fiberglass-reinforced-polyester laminate to meet the program's fragmentation requirements

2. 2 inches of lightweight aluminum honeycomb core (6.9 pounds per cubic foot) in an effort to balance the blast and fragmentation resistance

3. 1/8-inch total thickness of aluminum or fiber-reinforced-epoxy

All the panels would be comparable in weight; however, the more complex configurations would require more steps to fabricate (for example, Configuration 3). Configurations 1 and 2 would weigh less than the others since fewer components would be used.

The anticipated flexural resistance-deformation curves for the five sandwich configurations and a 1/2-inch sheet of GRP are shown in Figure 35. Configuration 4 yielded the greatest level of structural resistance and the greatest amount of strain energy absorption. However, Configurations 2 and 3 (if adhesive problems were solved) would satisfactorily withstand most weapon threats. They also offer the advantage of symmetry; that is, the structural module should be capable of resisting weapon blast and fragmentation equally well on both sides of the sandwich panel.

SUMMARY

The delamination mechanism, which is promoted by low-resin content and starch binder on the fiberglass, made the fiberglass-reinforced-polyester laminate a superior antifragmentation material. However, this property limited the laminate's structural capability. In each stress mode, the laminate's elasticity was limited by the strength characteristics of the polyester resin matrix. In the compressive, flexural, and laminating shear modes, the resistance could not be transferred from the polyester to the glass fiber reinforcement because the former deteriorates, initiating the failure of the laminate. However, the laminate tensile strength was over three times the stress level at which the polyester material started to break down because the fiberglass was capable of resisting much higher tensile loads. Thus the membrane tensile stress mode represented the most efficient mode of loading the laminate.

The strength of the laminate was found to deteriorate with water absorption because of the laminate's low resin content and starch binder. For field employment the GRP must be protected from moisture absorption by sealing all exposed edges.

The laminate material was demonstrated to be more structurally resistant when employed in sandwich configurations with the GRP serving as membrane facings on lightweight aluminum honeycomb core. However, sandwich construction inherently increases fabrication costs and shipping cube—two undesirable factors that could make this type of construction prohibitive for certain structural configurations such as highly mobile low cost personnel protection. Some of the sandwich configurations presented in this report utilized aluminum or fiber-reinforced epoxy sheets to aid the GRP in the compressive stress mode. Each configuration provided a level of structural resistance that was dependent upon the arrangement of the sandwich facings.

In permanent or semipermanent advanced bases symmetrical sandwich Configurations 2 and 3 are recommended for use in protective structural modules since each is capable of resisting the same blast pressure and fragmentation striking either side of the sandwich. Configuration 2 is recommended for short-term, lower structural loading and for upgrading the protection level of existing structures. Configuration 3 is recommended for construction modules which are to be subjected to long-term, higher structural loading where creep is also considered detrimental. Although the addition of an aluminum sheet to the GRP facings increased cost and weight, it was necessary in order that the panel's compressive face could resist high blast pressures and so that creep due to long-term loading could be eliminated.

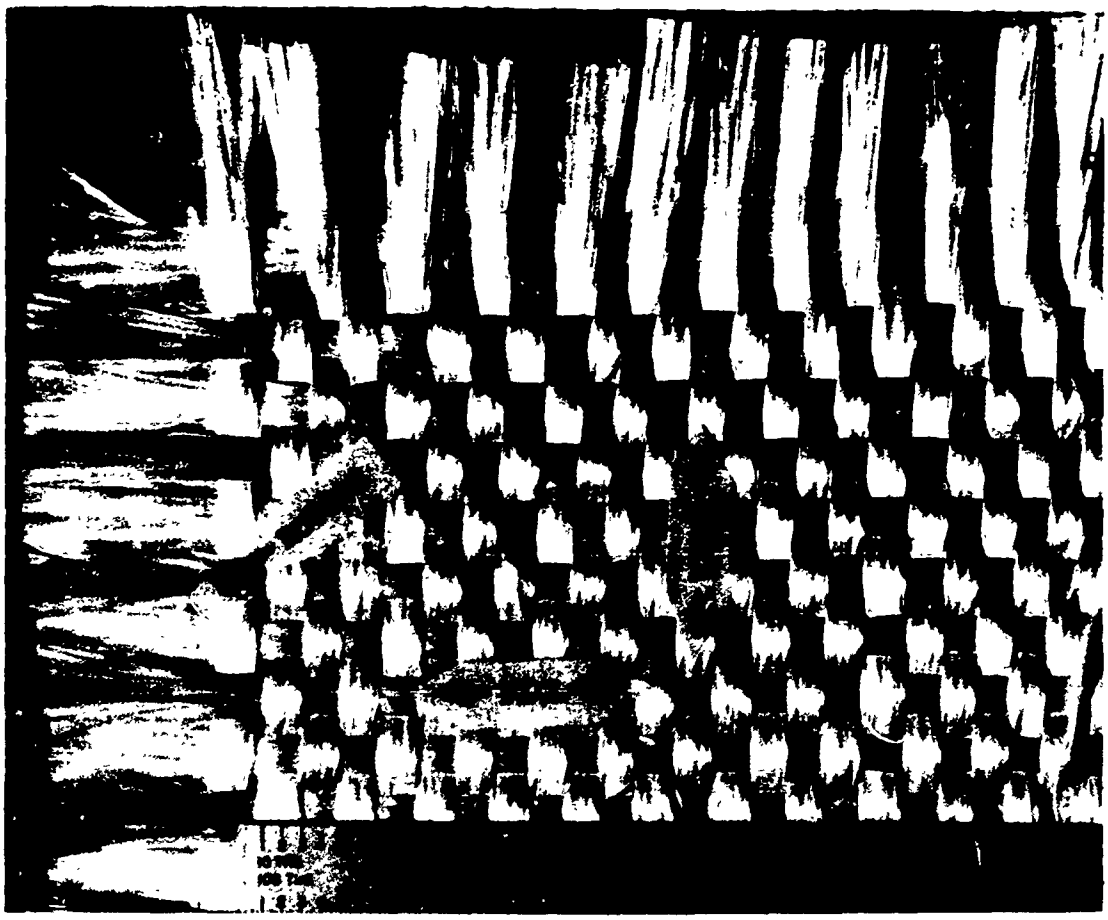

Figure 1. Woven-roving fiberglass cloth used to reinforce polyester resin. Arrows on warp and fill indicate direction of warp and fill rovings.

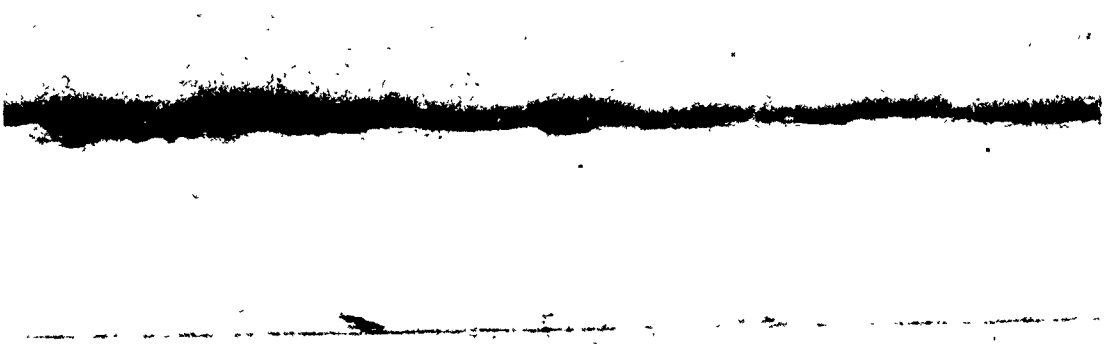

Figure 2. Cross section of 1/4-inch GRP laminate.

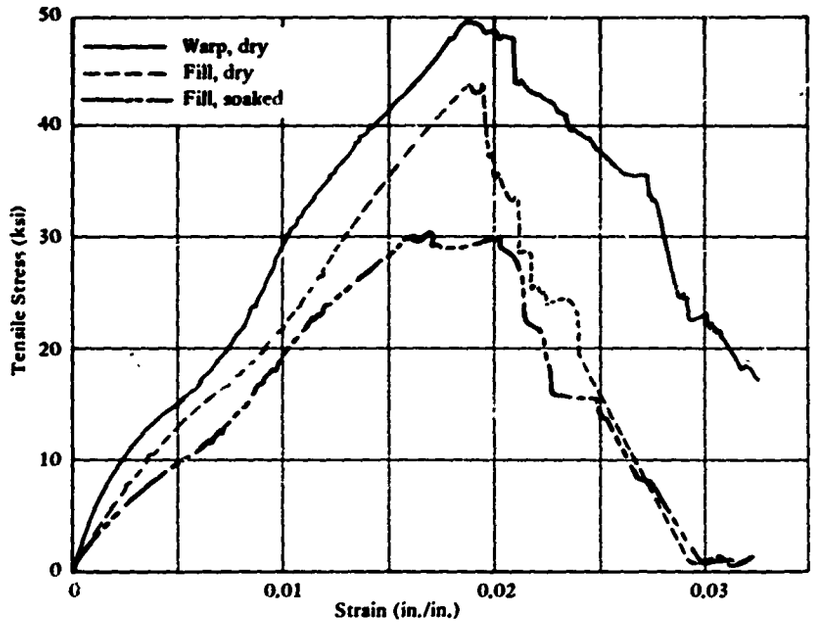

Figure 3. Example of stress-strain relationships in tension with 1/4-inch-thick GRP laminate.

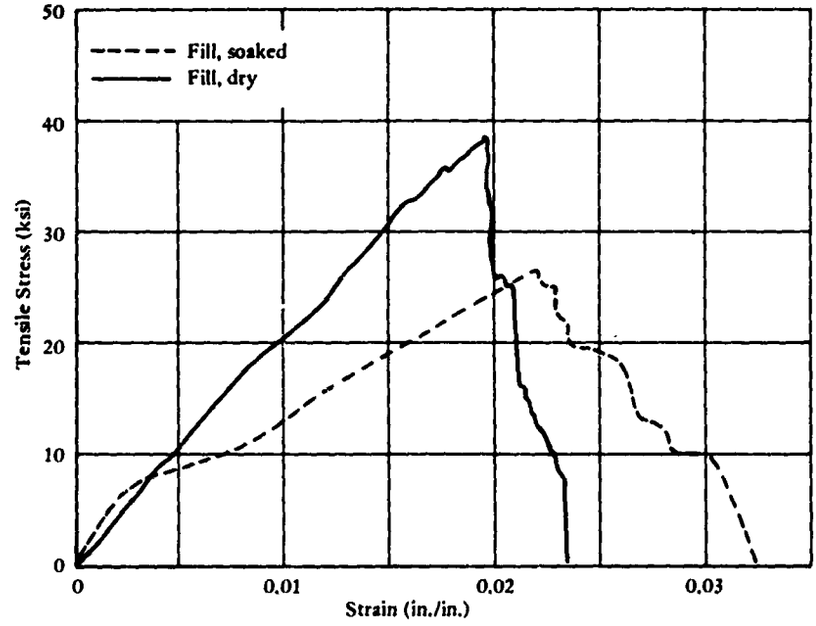

Figure 4. Example of stress-strain relationship in tension with 1/8-inch-thick GRP laminate.

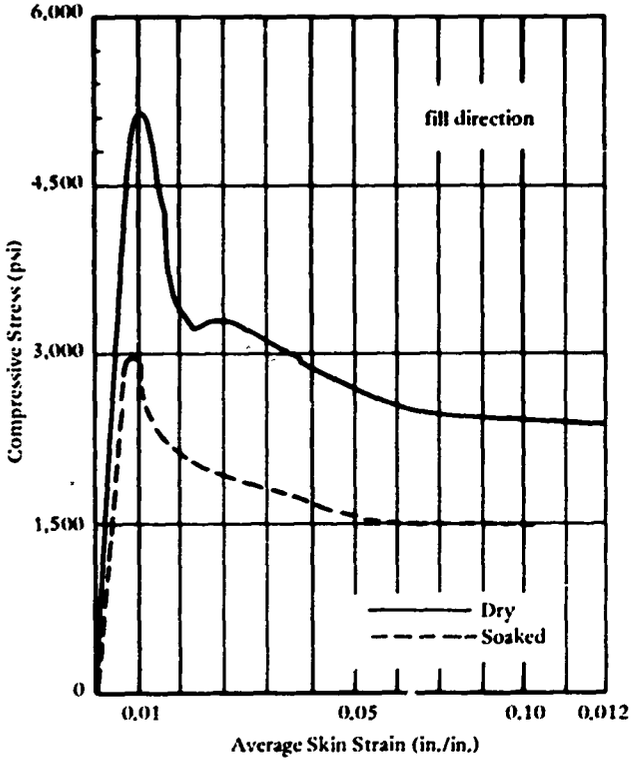

Figure 5. Example of stress-strain relationship in compression with 1/4-inch-thick GRP.

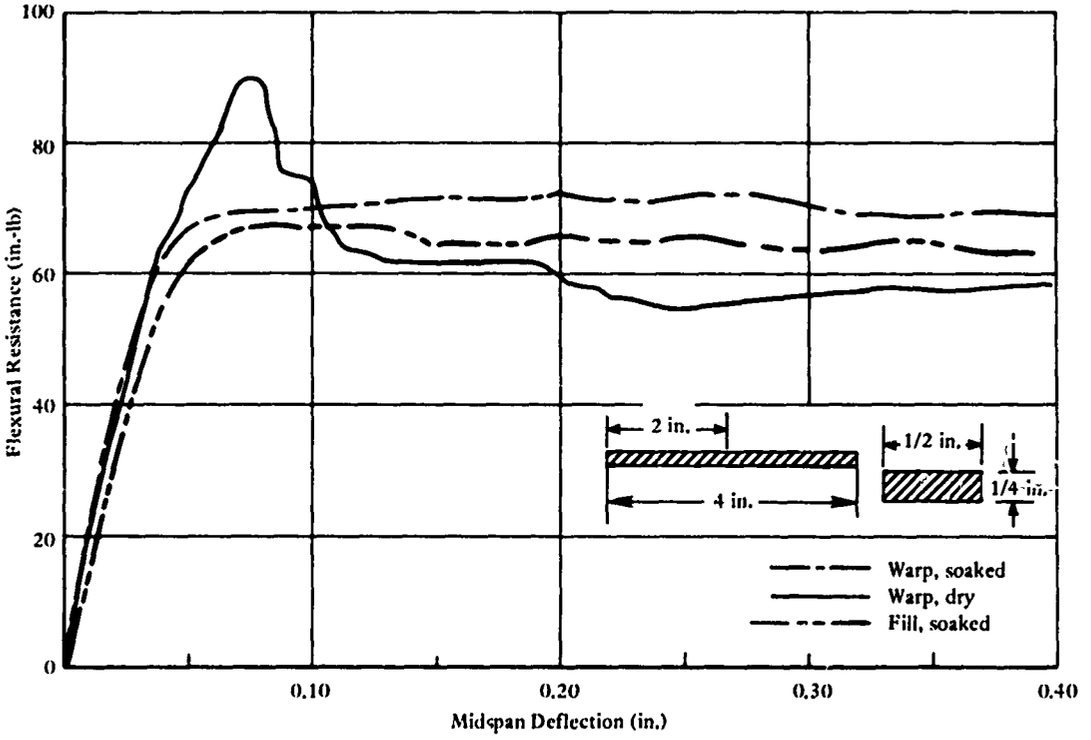

Figure 6. Example of coupon resistance-deflection relationship in flexure with 1/4-inch-thick GRP laminate.

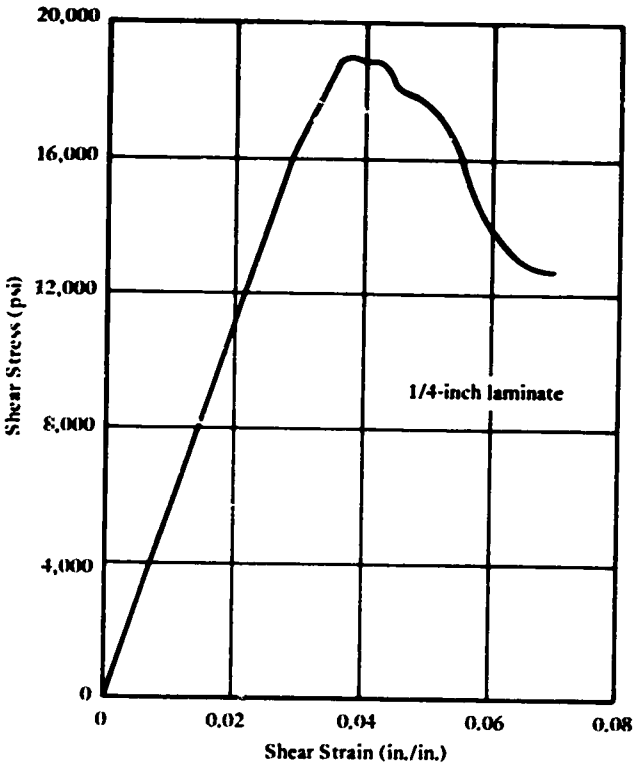

Figure 7. Example of shear stress-deformation curve for punching shear.

Figure 8. Coupon specimen showing delaminated resin and rupture of fiberglass strands sustained during tensile test.

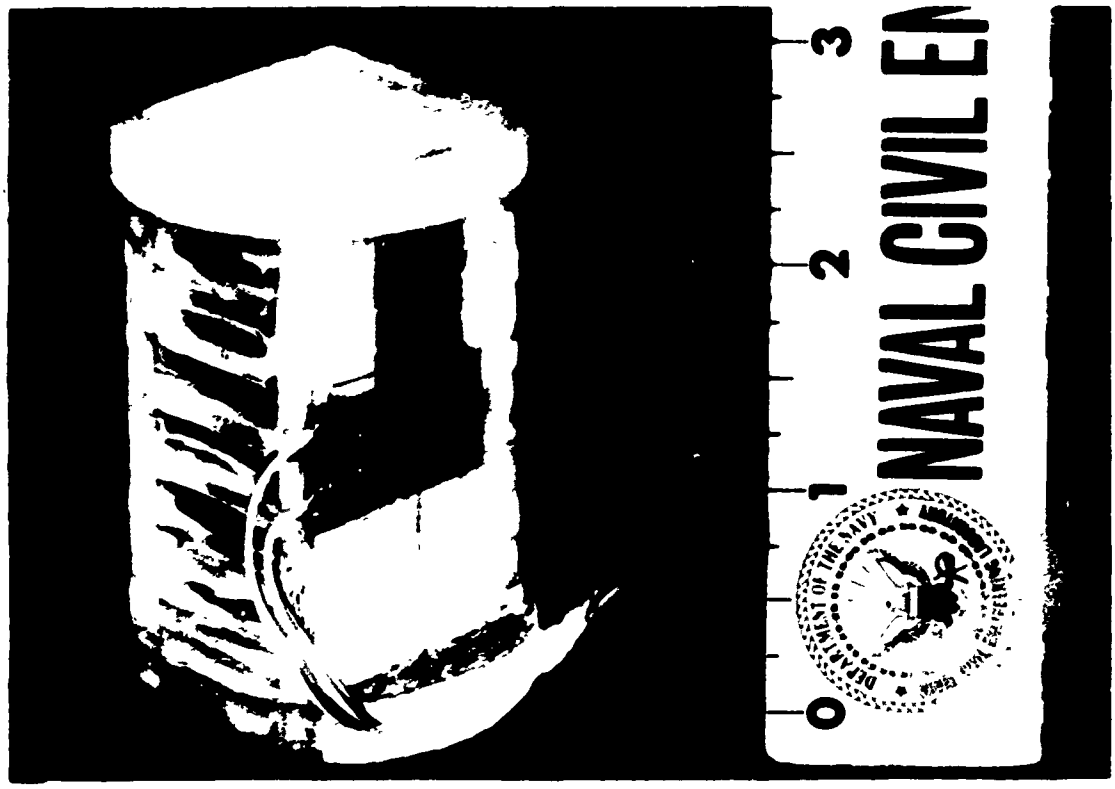

Figure 9. Compression coupon specimen strain-gaged to obtain Poisson's ratio.

Figure 10. Coupon specimen showing failure during compression test.

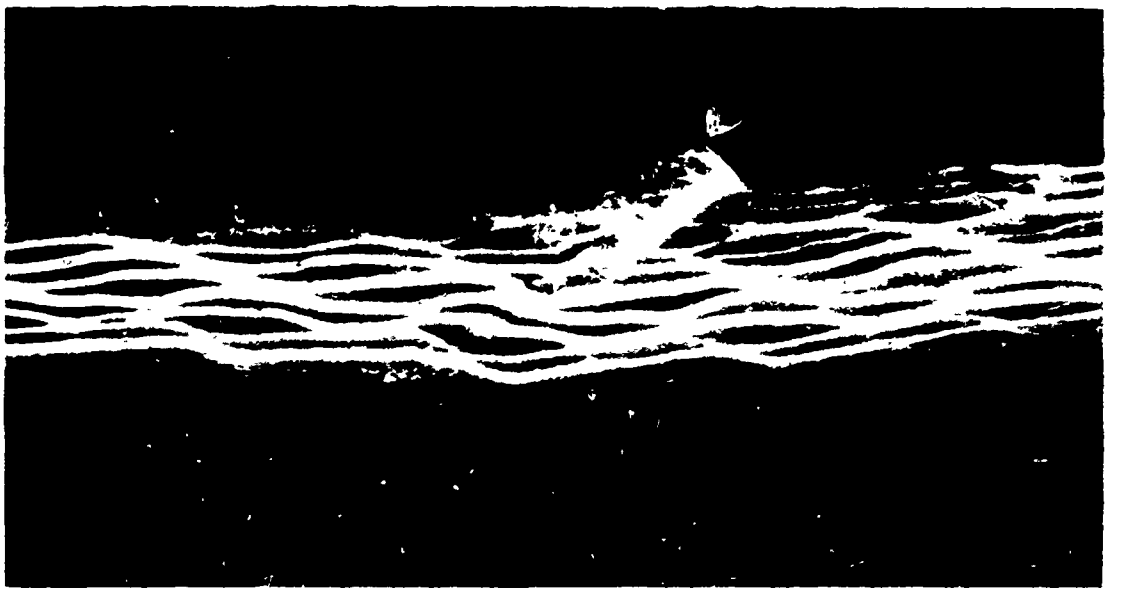

Figure 11. Coupon specimen showing failure during flexural test.

Figure 12. Coupon specimen showing failure during lamination shear test.

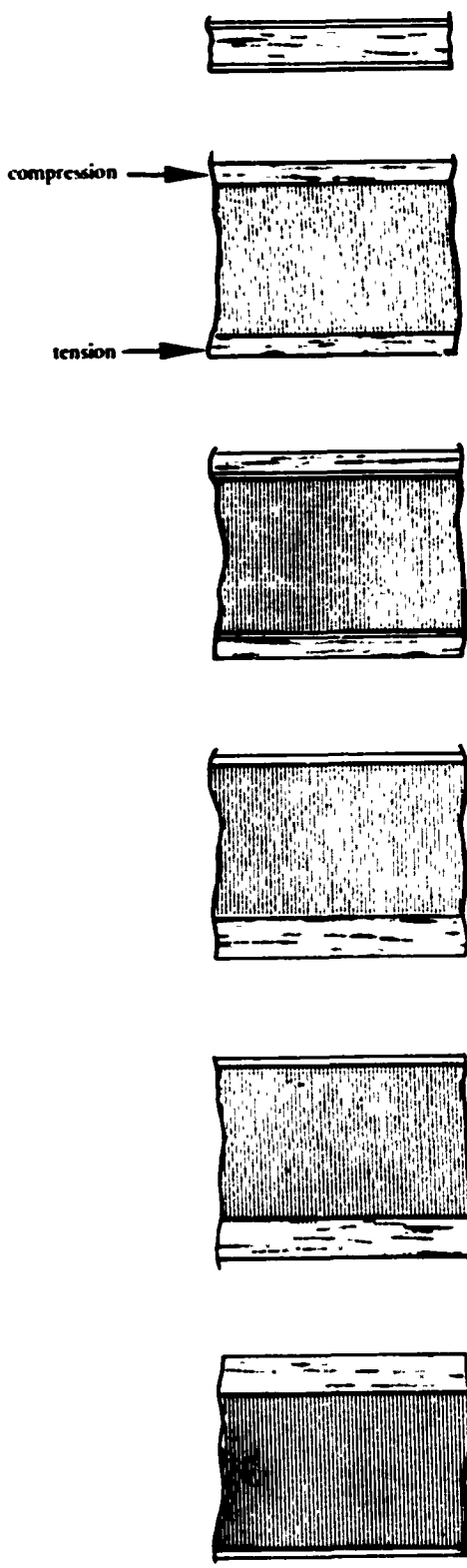

Configuration 1: GRP core with aluminum facings.

Configuration 2: aluminum honeycomb core with GRP facings.

Configuration 3: aluminum honeycomb core with composite GRP-aluminum facings.

Configuration 4: aluminum honeycomb core with aluminum sheet on compression side and GRP sheet on tension side.

Configuration 5: aluminum honeycomb core with sheet of fiber-reinforced-epoxy on compression side and GRP sheet on tension side.

Configuration 6: aluminum honeycomb core with GRP sheet on compression side and aluminum sheet on tension side (inverse of Configuration 4).

Figure 13. GRP composite sandwich configurations. In all cases, compression side is upper face, and tension side is lower face, as shown with Configuration 2.

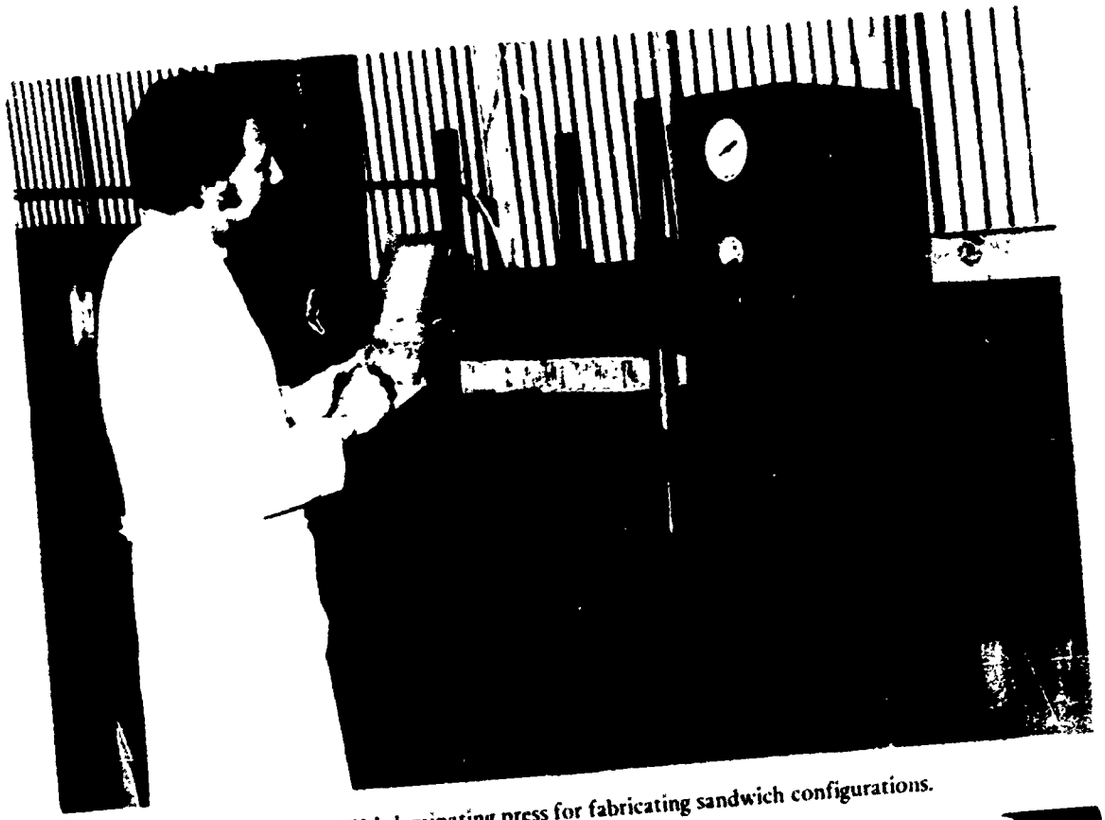

Figure 14. CEL's laminating press for fabricating sandwich configurations.

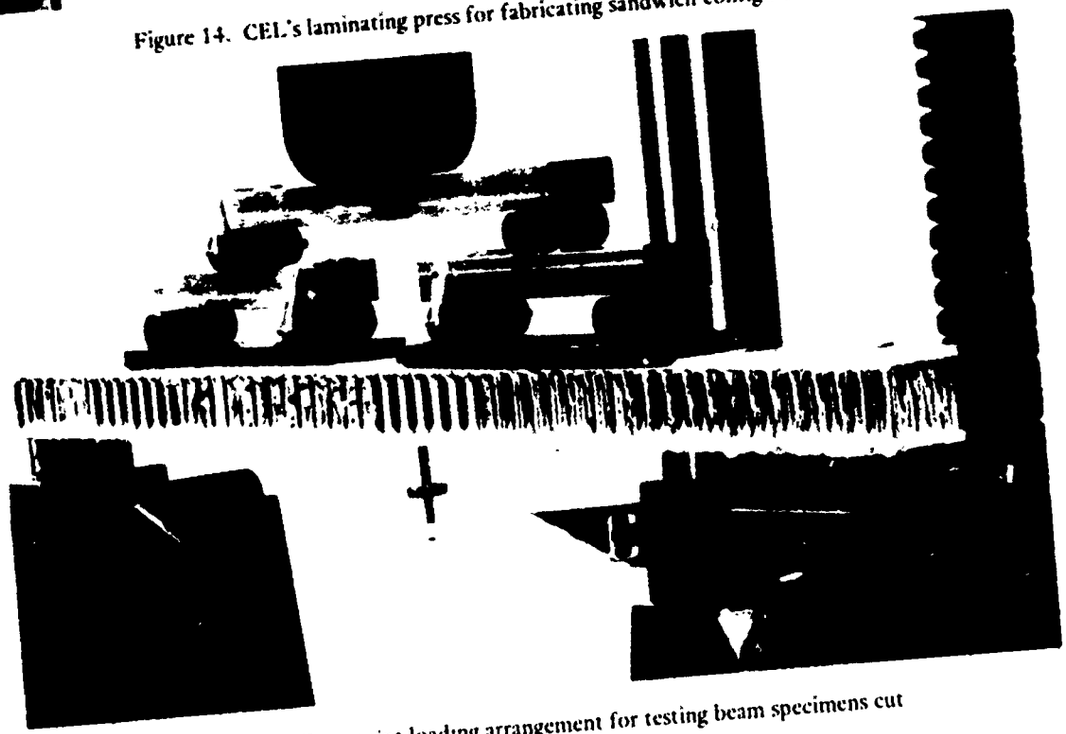

Figure 15. Four-point loading arrangement for testing beam specimens cut from sandwich configurations.

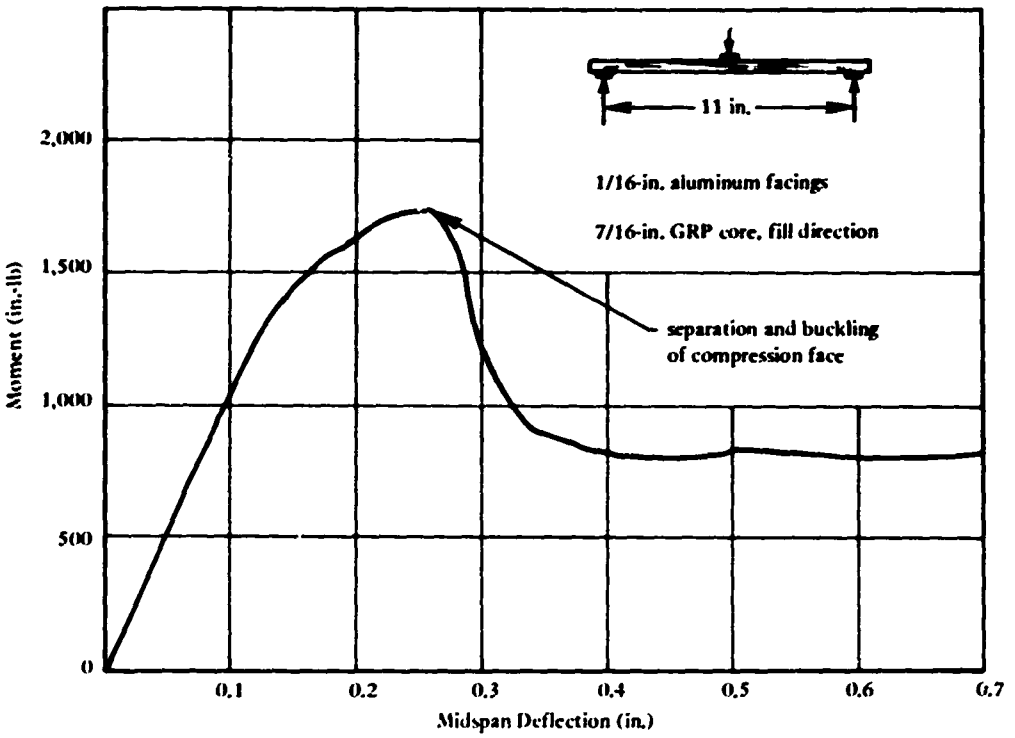

Figure 16. Moment-deflection curve for sandwich Configuration 1.

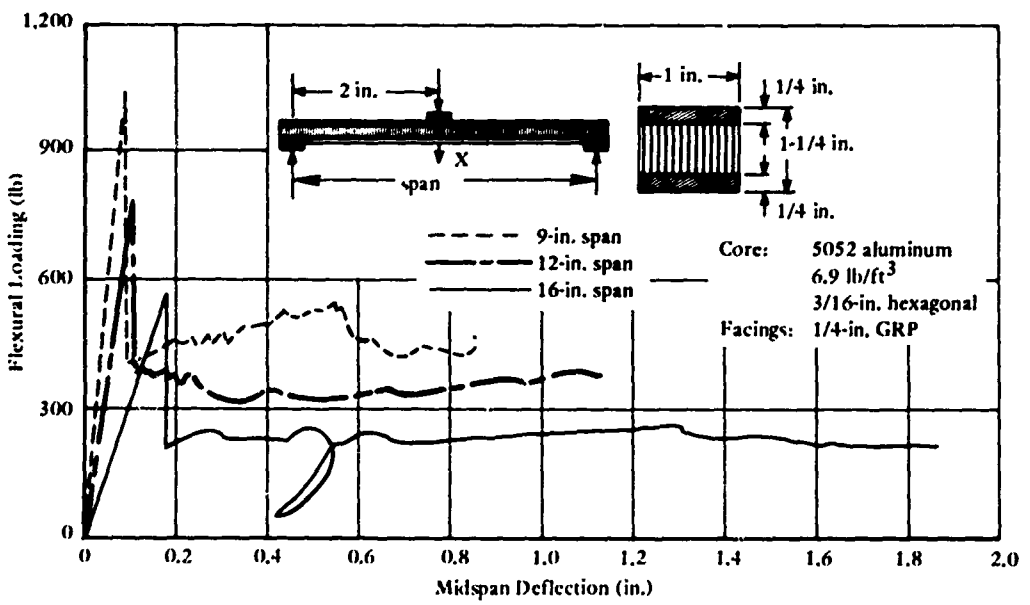

Figure 17. Typical resistance-deflection relationship in flexure, Configuration 2.

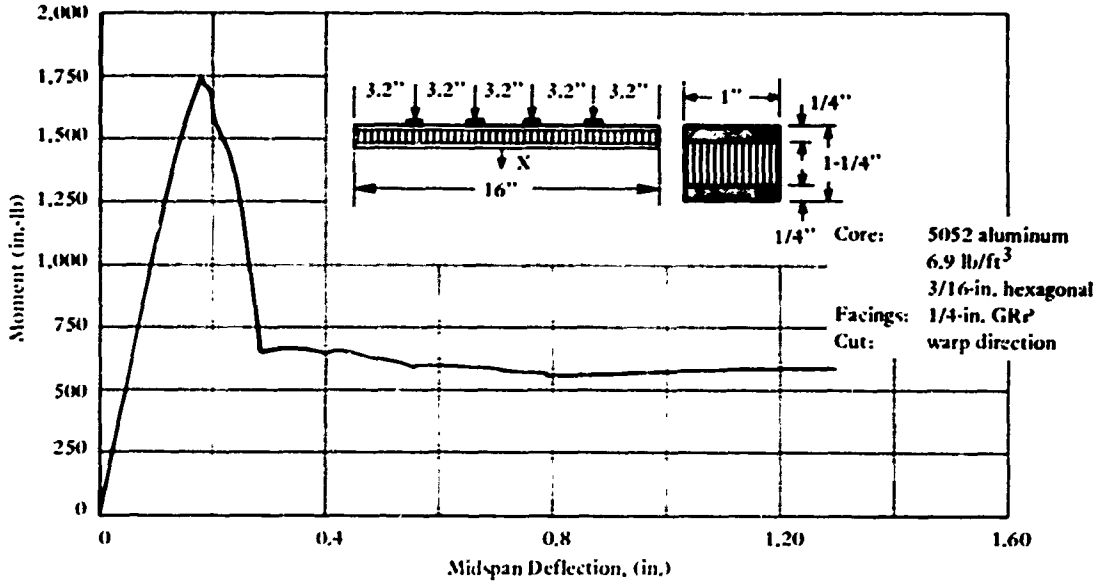

Figure 18. Typical resistance-deflection relationship in flexure, four-point loading, Configuration 2.

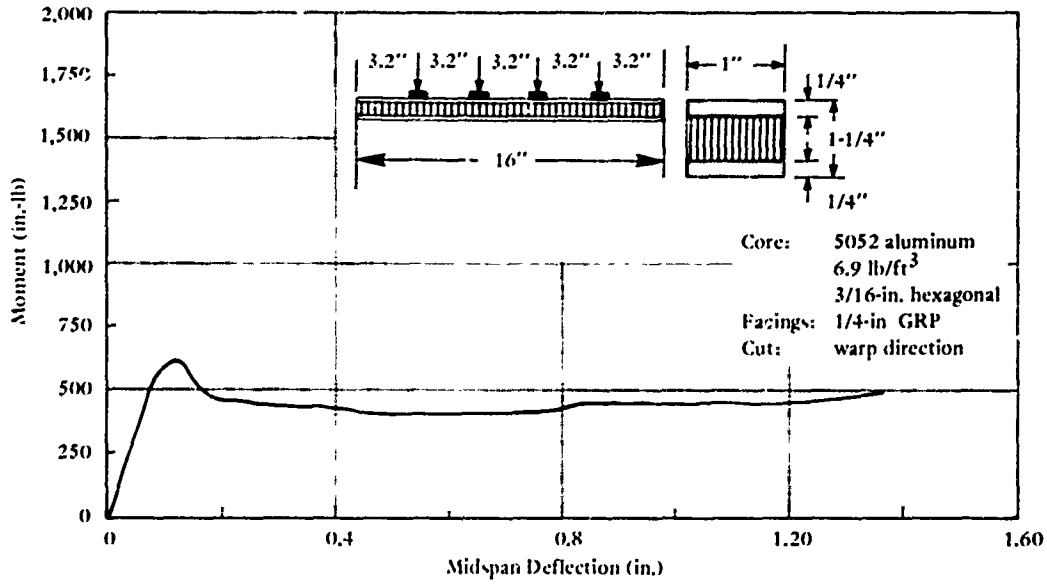

Figure 19. Typical uniform resistance-deflection relationship in flexure, Configuration 2, immersed in water 24 hours.

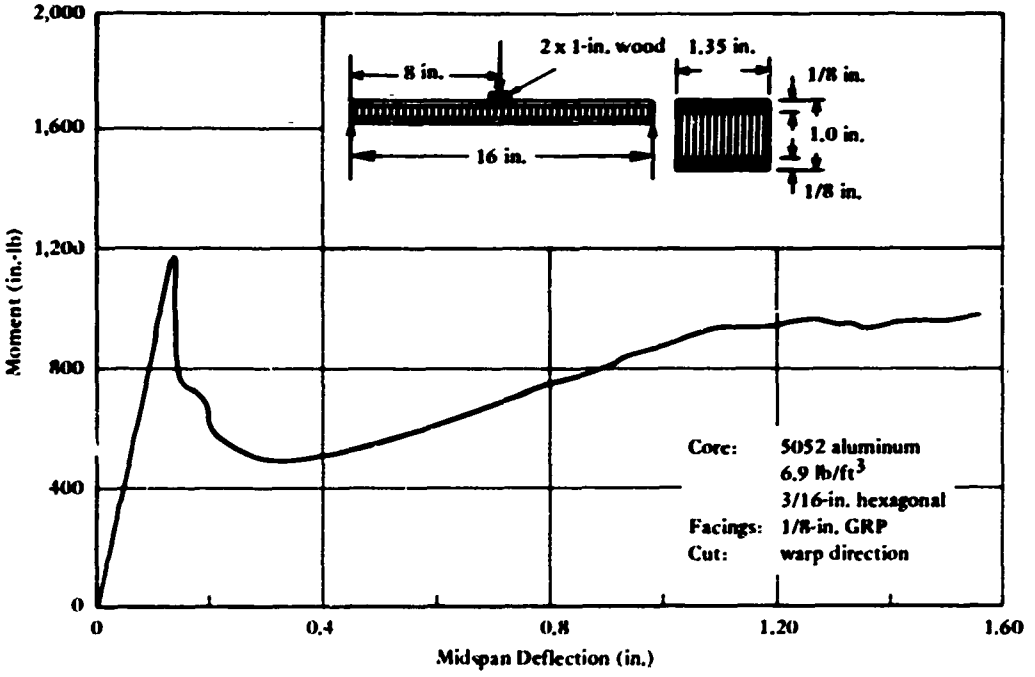

Figure 20. Typical resistance-deflection relationship in flexure, Configuration 2.

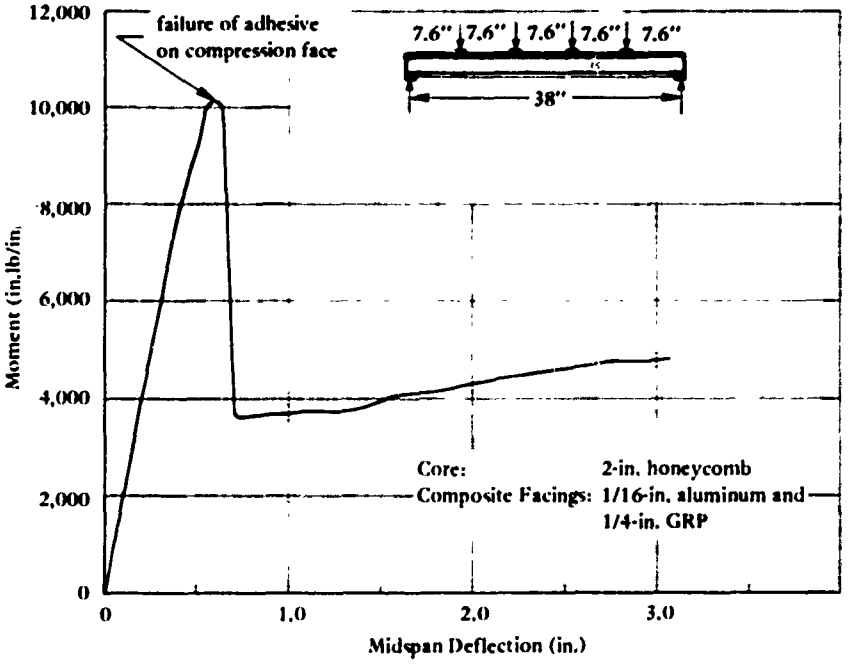

Figure 21. Sample moment-deformation curve, Configuration 3.

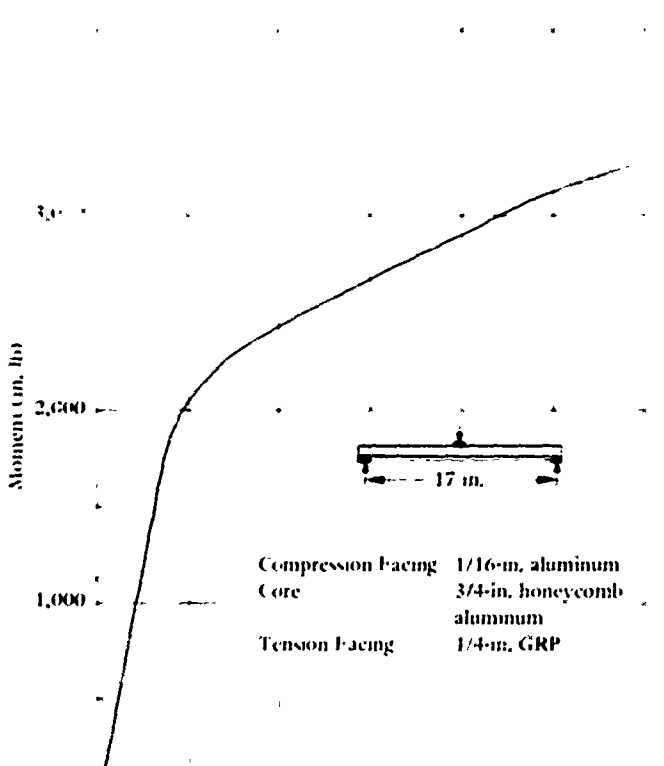

Figure 22. Sample moment-deflection curve, Configuration 4.

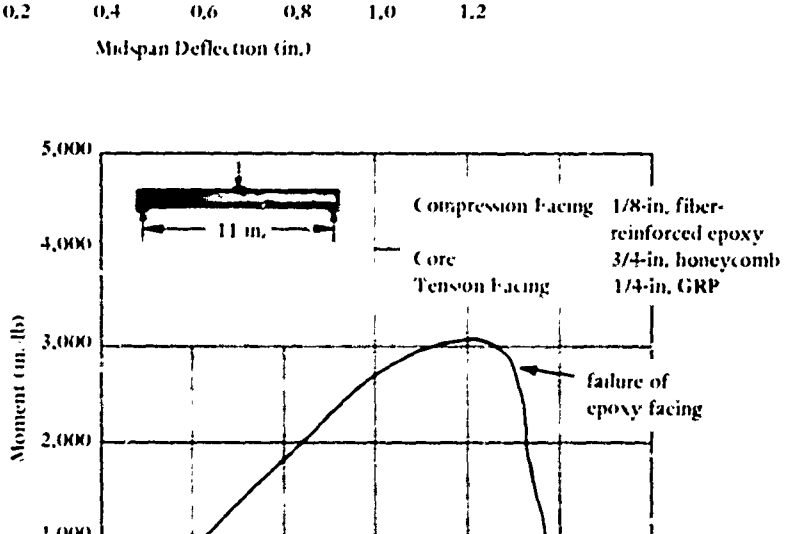

Figure 23. Moment-deflection curve, Configuration 5.

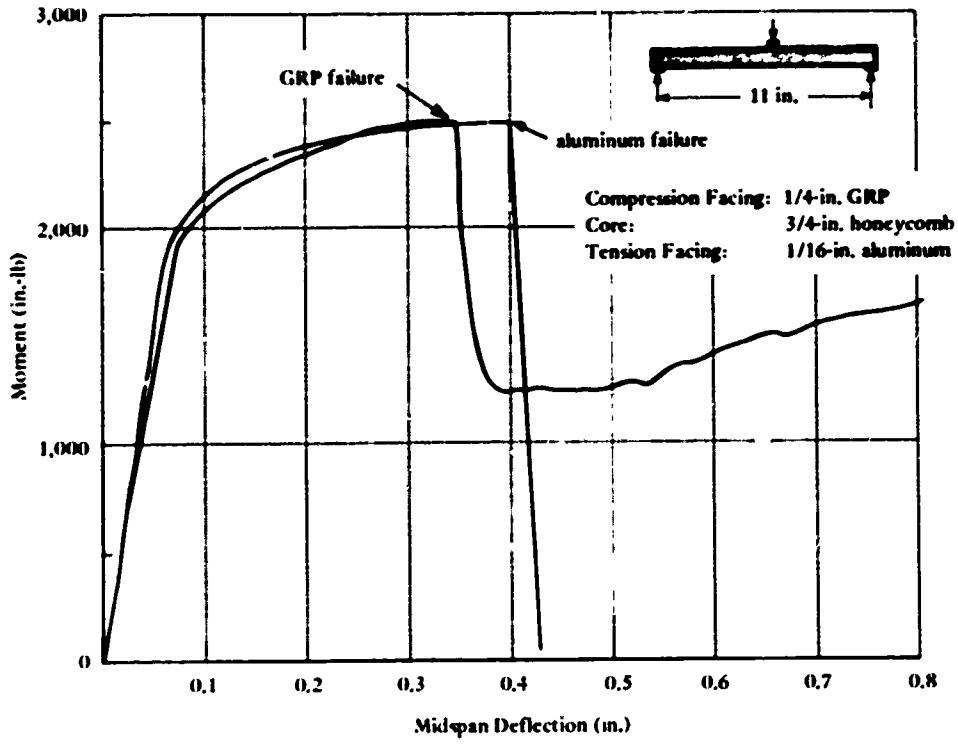

Figure 24. Moment-deflection curve, Configuration 6.

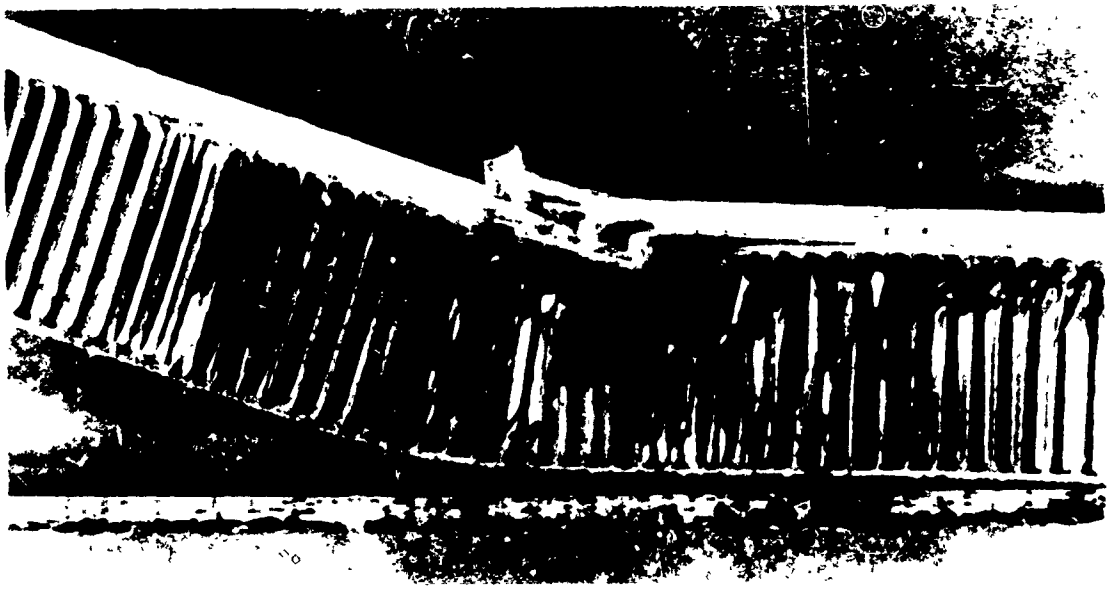

Figure 25. Buckling failure of aluminum and GRP due to inadequate adhesion between sandwich components, Configuration 3.

Figure 26. Failure due to delamination of sandwich facings, Configuration 5.

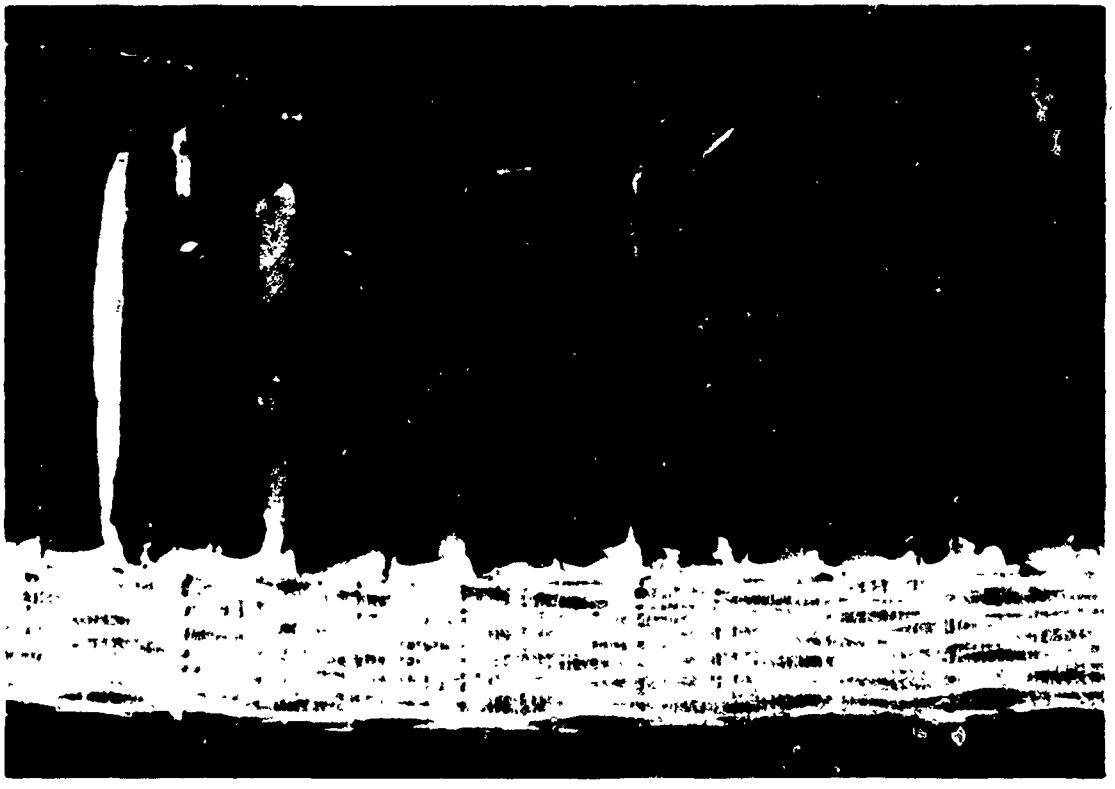

Figure 27. Crushing of aluminum honeycomb core beneath load, flexural specimen, Configuration 4.

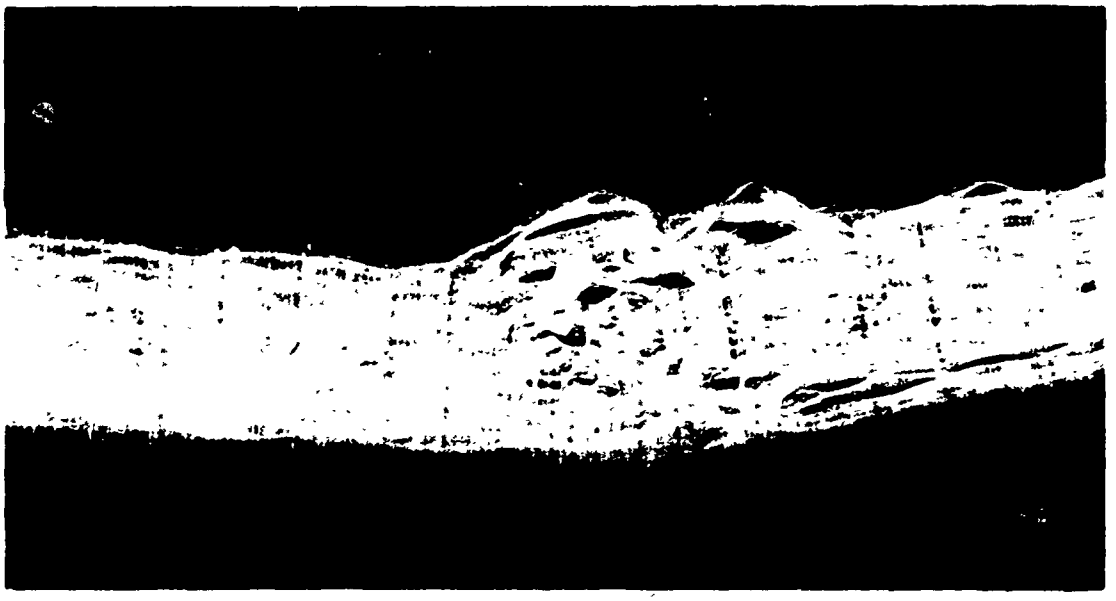

Figure 28. Failure of sandwich Configuration 1, flexural specimen.

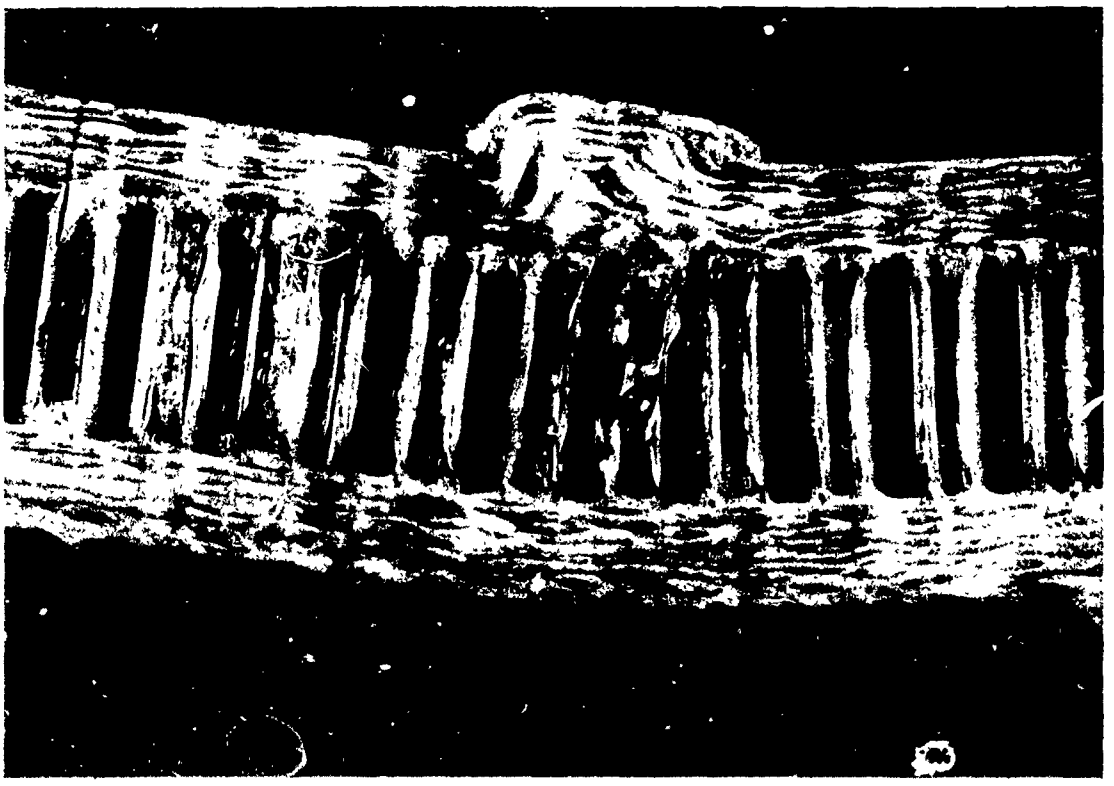

Figure 29. Failure of compression facing of GRP (typical failure, Configuration 2).

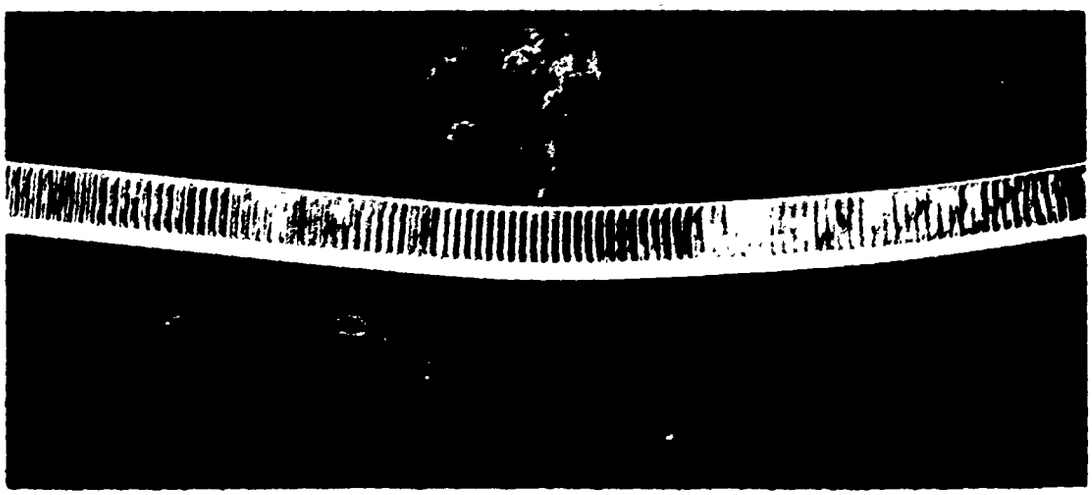

Figure 30. Permanent flexural deformation of beam specimen of Configuration 3.

Figure 31. Failure of the fiberglass-reinforced epoxy compression facing (typical failure, Configuration 5).

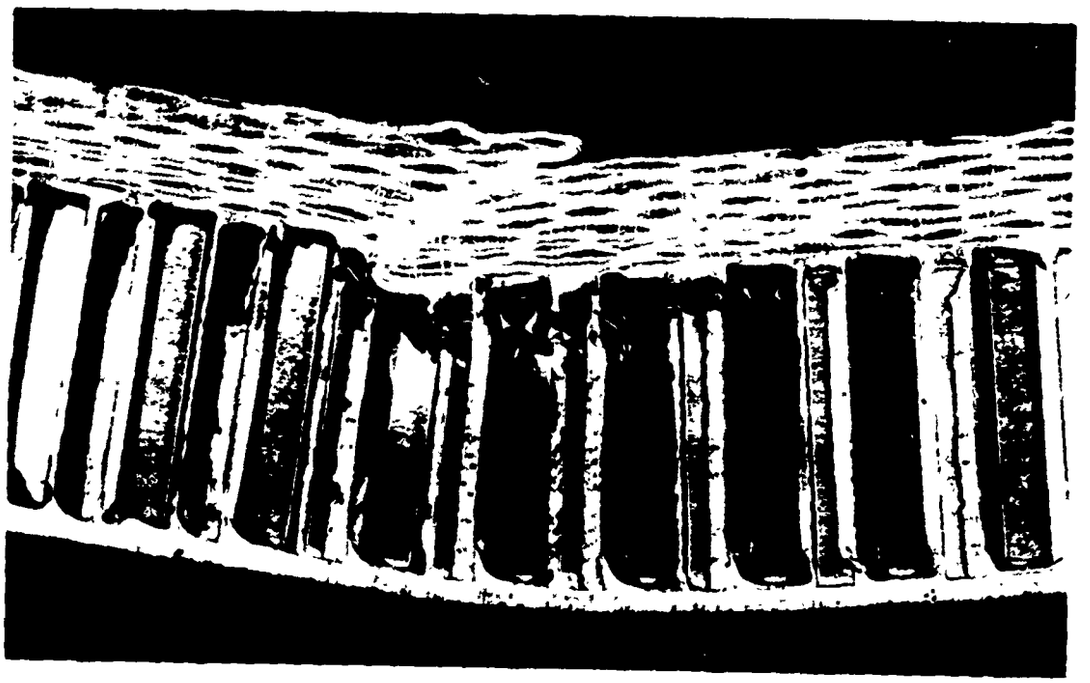

Figure 32. Failure of the GRP compression facing (beam specimen, Configuration 6).

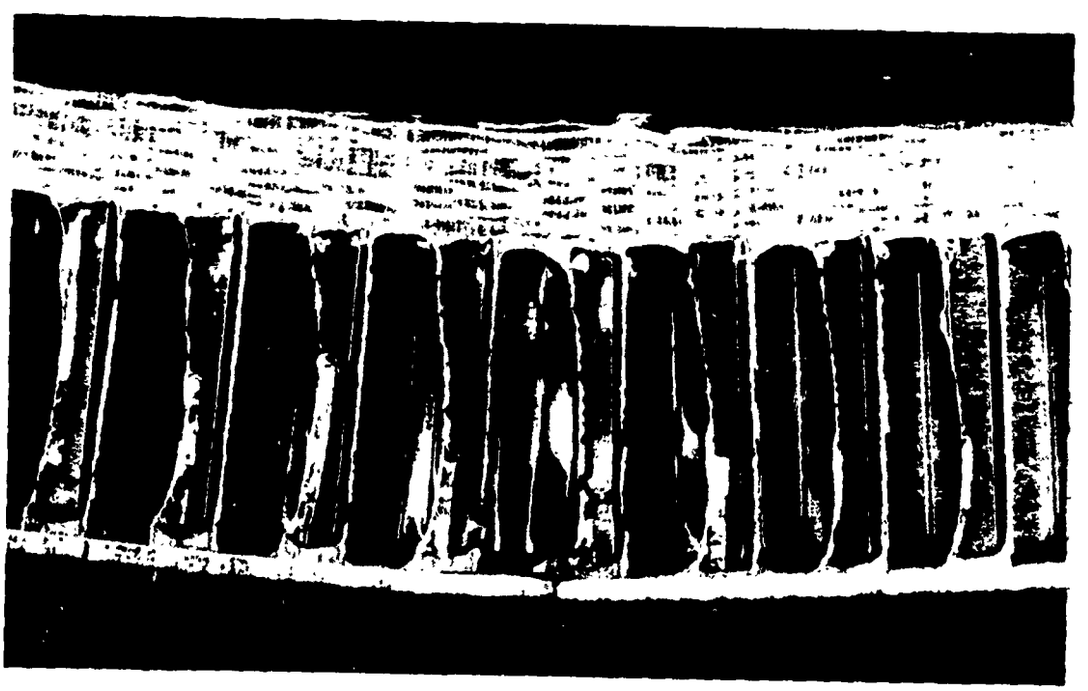

Figure 33. Failure of the aluminum tensile facing (beam specimen, Configuration 6).

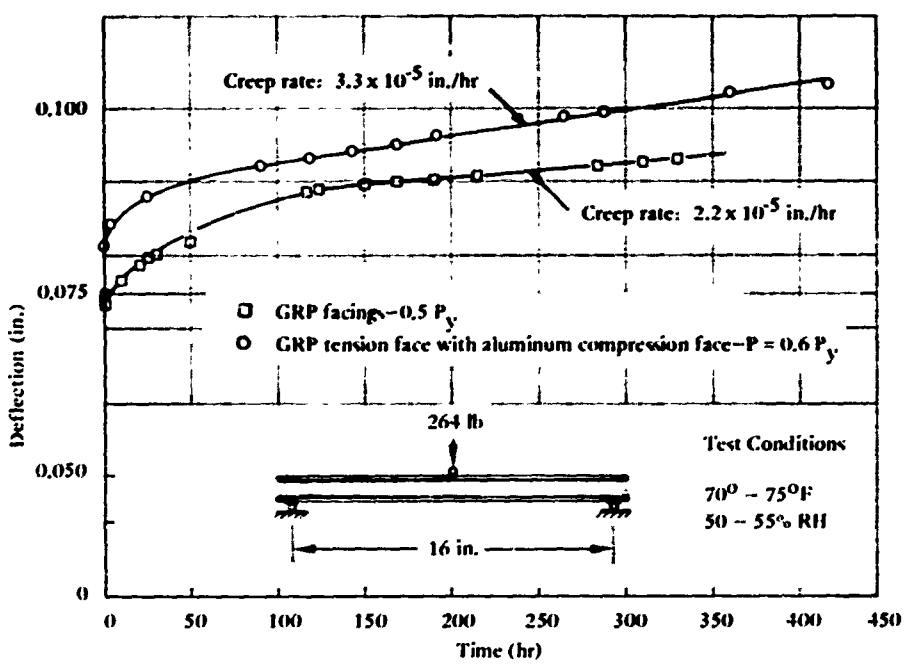

Figure 34. Creep test results with Configurations 2 and 4.

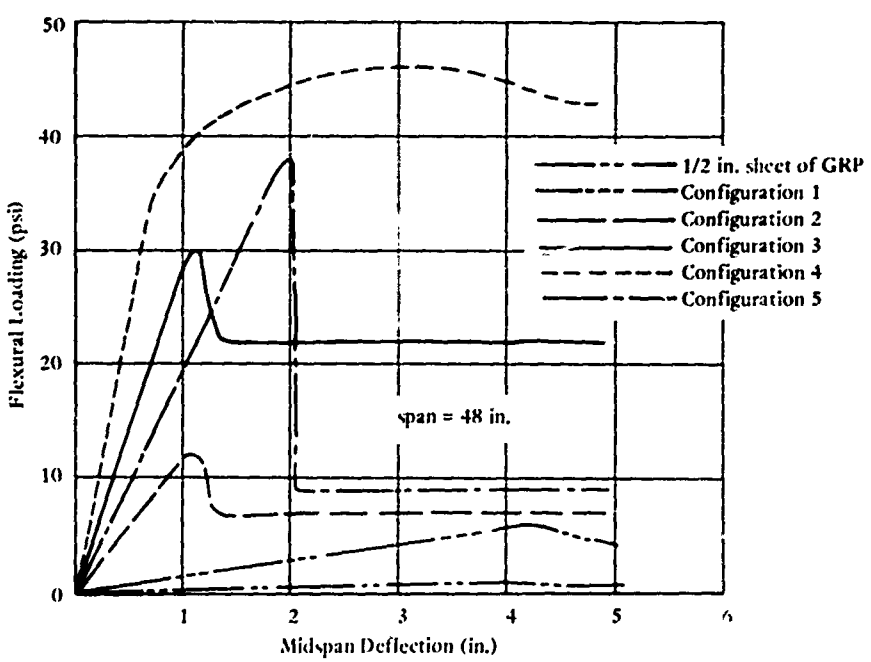

Figure 35. Resistance-deflection curves for candidate sandwich modules.

REFERENCES

1. Naval Civil Engineering Laboratory. Technical Report R-770: Prefabricated panels for rapid fortification by mobile marine forces, by C. E. Parker. Port Hueneme, CA., July 1972.

2. Technical Note N-1226: Tests of bonded woven roving, ballistic nylon, and sand against 81mm, 105mm, and 155mm projectiles, by W. A. Keenan. Port Hueneme, CA. June 1972.

3. Modern Plastics Encyclopedia. New York, McGraw-Hill, October 1972, Vol. 49, No. 10A., pp. 192-193.